

Intraseasonal variability in the Makassar Strait thermocline

by Kandaga Pujiana^{1,2}, Arnold L. Gordon¹, Janet Sprintall³ and R. Dwi Susanto¹

ABSTRACT

Intraseasonal variability [ISV] in the Makassar Strait thermocline is examined through the analysis of along-channel flow, regional sea level anomaly and wind fields from January 2004 through November 2006. The dominant variability of 45–90 day in the Makassar Strait along-channel flow is horizontally and vertically coherent and exhibits vertical energy propagation. The majority of the Makassar ISV is uncoupled to the energy exerted by the local atmospheric ISV; instead the Makassar ISV is due to the combination of a remotely forced baroclinic wave radiating from Lombok Strait and deep reaching ISV originating in the Sulawesi Sea. Thermocline depth changes associated with ENSO influence the ISV characteristics in the Makassar Strait lower thermocline, with intensified ISV during El Niño when the thermocline shallows and weakened ISV during La Niña.

1. Introduction

The flow through Makassar Strait represents the primary inflow gateway of the Pacific water composing the Indonesian Throughflow [ITF] (Fig. 1; Gordon and Fine, 1996). Gordon *et al.* (1999; 2008) showed that the Makassar throughflow is thermocline intensified, seasonally dependent, and modulated by El Niño-Southern Oscillation [ENSO] signals. Additionally, there are energetic fluctuations at tidal and intraseasonal [<90 day period] time scales (Susanto *et al.*, 2000).

The intraseasonal variability [ISV] within the atmosphere is a prominent feature of tropical climate, particularly in the region affected by the Asian and Australian-Indonesian monsoons (McBride and Frank, 1996). Two primary elements of ISV of the tropical atmosphere are the Madden-Julian Oscillation (MJO) and the convectively coupled equatorial Rossby waves (Madden and Julian, 1971; Wheeler *et al.*, 2000). Variances of MJO and equatorial Rossby waves are confined within the period bands of 30–80 days and 10–40 days respectively, and the motions of both features are primarily zonal in direction.

The oceanic ISV of the ITF is influenced by the remote wind variation in the Indian Ocean (Sprintall *et al.*, 2000; Wijffels and Meyers, 2004) and the Pacific Ocean (Cravatte *et al.*, 2004; Qu *et al.*, 2008). For example, relaxation of the southward flow within Makassar Strait with current reversal in the lower thermocline during the monsoon

1. Lamont Doherty Earth Observatory, Columbia University, Palisades, New York, 10964, U.S.A.

2. Corresponding author. *email:* kandaga@ldeo.columbia.edu

3. Scripps Institution of Oceanography, University of California, La Jolla, California, 92093, U.S.A.

transition period [April/May and October/November] is considered to be an intrusion of Indian Ocean semi-annual coastal Kelvin waves [CTKW] (Sprintall *et al.*, 2000; Syamsudin *et al.*, 2004; Iskandar *et al.*, 2005). Intraseasonal variability within the ITF inflow portal may also be indirectly influenced by the tropical intraseasonal wind in the Pacific Ocean. Cravatte *et al.* (2004), utilizing altimeter data, demonstrated the dynamics of intraseasonal Rossby waves that likely imposed perturbations to the low latitude boundary currents in the Western Pacific Ocean. It has also been suggested that semi-annual Rossby waves originating in the central tropical Pacific force semiannual variation of Mindanao Current (Qu *et al.*, 2008). In addition to the ISV drawing most of its momentum from remote atmospheric perturbations, ISV formed within the Sulawesi Sea due to baroclinic Rossby wave resonance may also inject ISV energy into the Makassar Strait (Qiu *et al.*, 1999; Masumoto *et al.*, 2001).

The Susanto *et al.* (2000) study of the intraseasonal variability in the Makassar Strait, using a 1.5 year (1996–1998) time series of currents at 300 m and 450 m, showed two significant ISV peaks: 35–60 and 70–100 days. They suspected that the 35–60 day oscillations are associated with the Sulawesi Sea ISV (Qiu *et al.*, 1999; Kashino *et al.*, 1999) while the 70–100 day oscillations are related to a Kelvin wave from the Indian Ocean (Qiu *et al.*, 1999; Sprintall *et al.*, 2000).

This study investigates ISV features within Makassar Strait throughout the full thermocline depth. We first describe the data and method employed. This is then followed by discussions on the intraseasonal characteristics within Makassar Strait and how they are related to ISV within Sulawesi Sea to the north and ISV in Lombok Strait to the south of Makassar Strait.

2. Data and method

The oceanic ISV characteristics in Makassar Strait were investigated through flow as recorded from two moorings: 2°51.9'S, 118°27.3'E [MAK-West] and 2°51.5'S, 118°37.7'E [MAK-East], within the 45 km wide Labani Channel (Gordon *et al.*, 2008; Fig. 1). Each mooring consisted of an upward-looking RD Instruments Long Ranger 75 kHz Acoustic Doppler Current Profiler [ADCP] at depth 300 m and two current meters deployed at 200 m and 400 m that measured the variation of zonal and meridional velocity. The zonal and meridional velocity data were linearly interpolated onto a 25-m depth grid for each two-hour time step to produce the gridded current vectors from 25 m to 400 m. These gridded current vectors were subsequently used to compute the along-channel flow parallel to the along axis of Labani Channel, which is oriented along 170°. To examine the links via Lombok Strait between the oceanic ISV recorded in Makassar Strait and that of the eastern equatorial Indian Ocean [EEIO], current meter data retrieved every two hours at 50 m and 350 m within Lombok Strait and at EEIO were analyzed. The data in Lombok Strait were recorded by the Lombok-East mooring deployed at 8°24.1'S, 115°53.9'E, north of 300 m sill (Sprintall *et al.*, 2009) and in the EEIO at 0°, 90°E (Masumoto *et al.*, 2005; Fig. 1). The time series, recovered from all moorings, extends from early January 2004 to late

November 2006 encompassing a period of weak El Niño from January 2004 until October 2005, followed by a La Niña until April 2006, with a mild El Niño until the end of observation period. The Makassar and Lombok moorings are part of the International Nusantara Stratification and Transport [INSTANT] program (Sprintall *et al.*, 2004).

The influence of remotely forced ISV to Makassar Strait ISV was evaluated using satellite altimeter JASON-1 derived Sea Level Anomaly [SLA] datasets in the Sulawesi Sea and Lombok Strait. The data were acquired from the database of sea-surface height recorded every 10 days along the Jason-1 satellite altimetry tracks [<http://podaac.jpl.nasa.gov/jason1>]. In the Sulawesi Sea, the along-track SLA data derived from several Jason satellite passes were interpolated through an inverse distance weighted [IDW] method to yield the estimated SLA data at 3°N along longitudes from 118°E to 125°E. The principle premise of the IDW method is that the interpolating data are weighted by the inverse of their distance to the interpolated data (Fisher *et al.*, 1987).

The atmospheric ISV in Makassar Strait was assessed through the analysis of the local wind variability. Wind data were collected from a wind gauge placed 10 m above mean sea level at Balikpapan airport (Fig. 1) and sampled every two hours coincident with the mooring time series.

Isolating the intraseasonal variability from the full datasets was accomplished using a cosine-recursive Butterworth filter, with a 20–90 day band pass window. The intraseasonal characteristics of the datasets were then examined using spectral, coherence, wavelet, wavelet coherence [<http://www.pol.ac.uk/home/research/waveletcoherence/>], and complex EOF analyses. To increase the statistical reliability of the spectral and coherence methods a multitaper analysis was applied. Multitaper analysis multiplies the overlapped and segmented data by several different windows or tapers and subsequently averages the estimates to get an averaged spectrum with a higher degree of freedom or smaller uncertainty (Percival and Walden, 1993). The type of orthogonal window applied in our study was the discrete prolate spheroidal sequence (Percival and Walden, 1993). The confidence levels, specified for the analysis involving spectral and coherence estimates, were computed based on the number of degrees of freedom or independent cross-spectral realizations in each frequency band (Thompson, 1979).

3. Intraseasonal features

a. ISV observed in the Makassar Strait

i. *Along-channel flow features.* ISV within the thermocline at Mak-West and Mak-East mooring sites is marked by oscillations within a wide spectrum of 45–90 days with a spectral peak at 60 days (Fig. 2 a,b,c,d). A second peak within a band of 30–40 days occurs at both moorings, but it is not significantly different from the background at the 95% confidence limits (Fig. 2 c,d). Figure 2 shows that the signature of the dominant ISV is characteristically stronger in the upper 100 m of water depth at both mooring sites, and it is discernable down to the base of the thermocline although with reduced energy. The

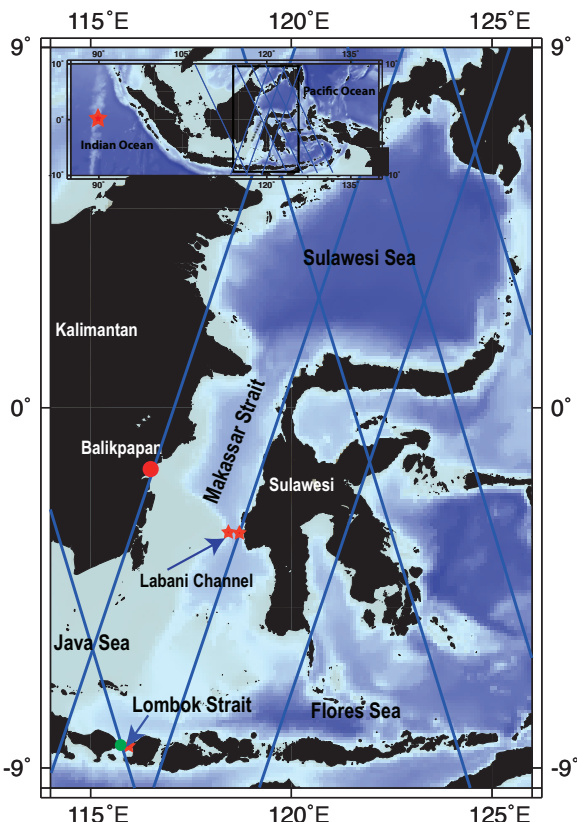


Figure 1. Mooring sites in Makassar Strait [Mak-West and Mak-East] and in Lombok Strait [Lom-East] are shown as red stars. Mak-West and Mak-East moorings were deployed in Labani channel, the narrowest deep passage in Makassar Strait, and separated by a distance of ~ 19 km. The red circle indicates location of the Balikpapan airport where the local wind data were measured. The blue lines denote the JASON-1 satellite altimetry tracks and the green circle indicates the site of a JASON-1 derived Sea Level Anomaly time series used in this study. Location of the eastern equatorial Indian Ocean mooring is shown as the red star in the insert.

Brunt-Väisälä frequency profiles (Fig. 3) at the Mak-West and Mak-East thermocline, inferred from several Conductivity-Temperature-Depth [CTD] casts carried out during the Northwest monsoon [rainy season], indicate that the strongest stratification is observed at depth between 100–125 m. This strong stratification demarcates the upper thermocline [25 m–100 m] from the lower thermocline [125 m–400 m] in Makassar Strait.

In the upper thermocline [25 m–100 m] the 60-day oscillation at Mak-West is a half order more energetic than that at Mak-East (Fig. 2 c,d), with 75% of the variance of both moorings being strongly coherent (Fig. 4, left panel). The coherence of the 60-day variability at both moorings attains its maximum value at 25 m and declines below the

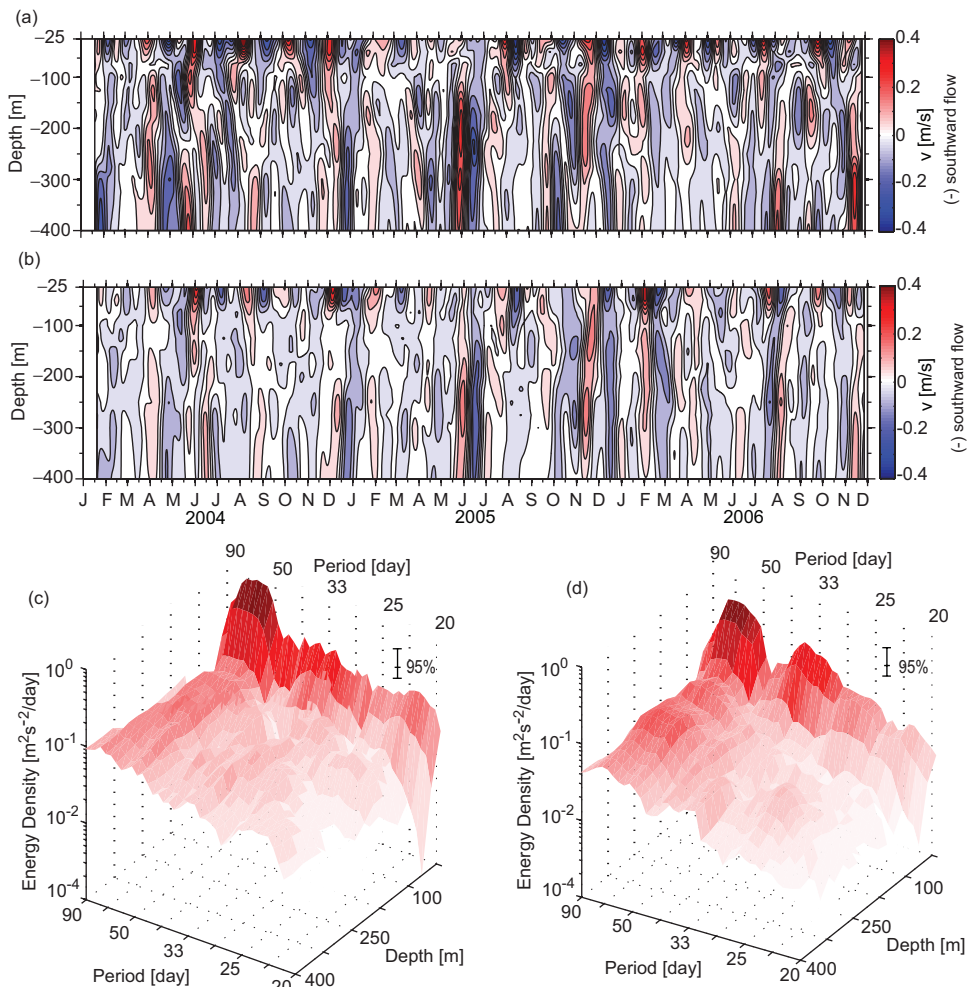


Figure 2. Along-channel thermocline flow at intraseasonal time scales observed at (a) Mak-West and (b) Mak-East. Negative values denote southward flow. (c,d) Spectral estimates of (a) and (b), respectively. Error bars on the spectral estimates mark the 95% confidence limits using power spectral confidence intervals (Jenkins and Watts, 1969).

significance level at 100 m. In terms of the relative phase relationship, the principal fluctuations in the upper thermocline of Mak-East lead that of Mak-West by 3°–19°, equivalent to 0.5–3 days; the lead is maximum at 25 m and minimum to 75 m (Fig. 4, right panel). The phase lag is unreliable at 100 m because the coherence squared is below the significance level at that depth.

Within the lower thermocline (125 m–400 m) the percentage of strongly correlated along-channel flow at Mak-West and Mak-East increases to 85% (Fig. 4). The horizontal

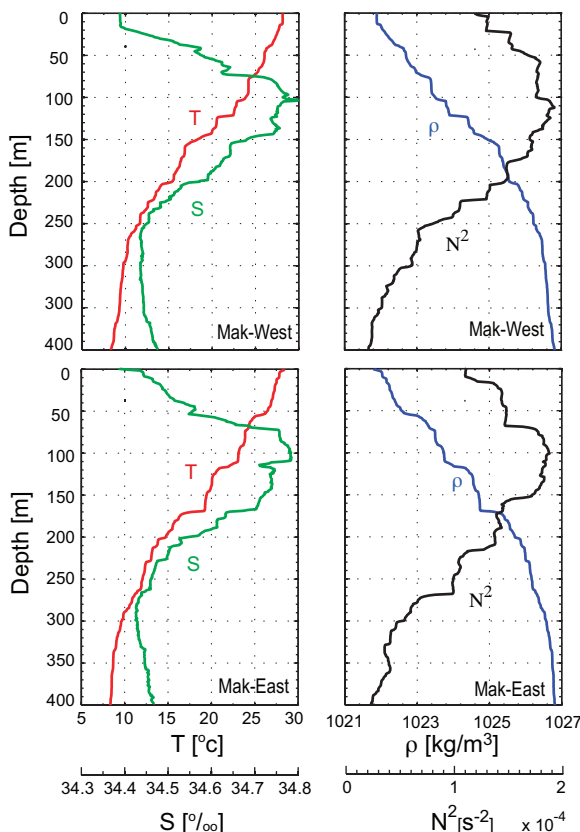


Figure 3. Temperature [red], Salinity [green], Density [blue], and Brunt-Väisälä [black] frequency profiles obtained from the CTD casts at the Mak-West [upper panel] and Mak-East [lower panel] mooring sites. The CTD data were collected in January 1994 during the Southeast monsoon.

coherence is minimum at 125 m and substantially increases toward the base of the thermocline at 400 m while the relative phase shift reveals the tendency of the ISV of Mak-West to lead that of Mak-East by 1-day. The zonally coherent along-channel flow at intraseasonal time scales as inferred from the two mooring sites is likely an indication that ISV length scale is much larger than the width separating the moorings.

We explored the vertical structure of ISV by considering the vertical coherence of intraseasonal along-channel flows at the Mak-West site. We focused on the Mak-West features and as Figure 4 shows, there is little difference between Mak-West and Mak-East at the ISV time scales that we are interested in. The results of a cross coherence method suggest that the significant 60-day upper thermocline feature is also quantitatively vertically coherent (Fig. 5a). The vertically coherent feature observed in the upper thermocline is particularly energetic in 2004 and 2006 and less vigorous during a weak El Niño period in the first six months of 2005 (Fig. 6a). We suggest that shear attenuation is

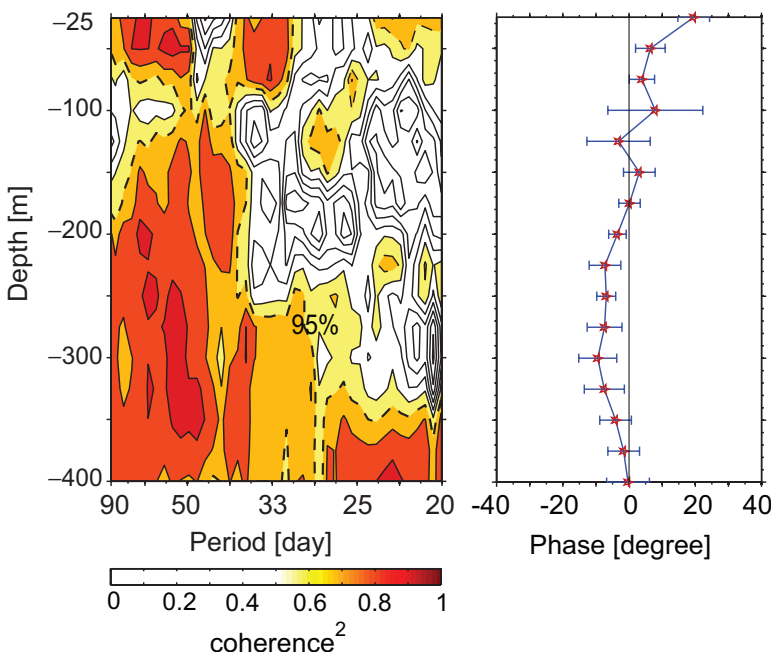


Figure 4. Coherence between the intraseasonal along-channel flow from Mak-West and Mak-East observed at the same depth. [Left panel]: Coherence squared. The dashed lines indicate the 95% significance level. [Right Panel]: Phase lags [stars]. Positive phases denote the intraseasonal along-channel flow at Mak-East leads the intraseasonal along-channel flow at Mak-West. Error bars show the 95% confidence limits for the phase lag estimates and were computed using a Monte-Carlo scheme.

due to the shoaling of the Makassar thermocline and less ITF transport during this El Niño phase (Gordon *et al.*, 1999; Ffield *et al.*, 2000). The weakening of the intraseasonal signatures in the upper thermocline was observed a couple of months after the sea surface temperature maximum marking the El Niño onset appeared in the central Pacific Ocean. The lag reflects the role of the baroclinic Rossby waves with a phase speed of 0.3 m/s that transmit variability in the central Pacific towards the western Pacific (Cravatte *et al.*, 2004) and eventually into Makassar Strait. In the lower thermocline, the coherence persists over all depths (Fig. 5b), and is consistently strong throughout the year (Fig. 6b).

Apart from the strong coherence, another feature of the lower thermocline is the pattern of phase lags. The phase relation between the ISV at 200 m and deeper layers shows a linear trend of the vertical phase lags in the lower thermocline with a slope of $11^\circ/50\text{ m}$ (Fig. 5b, right panel). The lags (Fig. 5b, right panel) signify that the vertically coherent signals found in the lower thermocline exhibit a two-day shift for every 50 m of increasing depth, and thus are indicative of downward energy propagation. Downward energy propagation is a common expression of waveform propagation in a stratified ocean

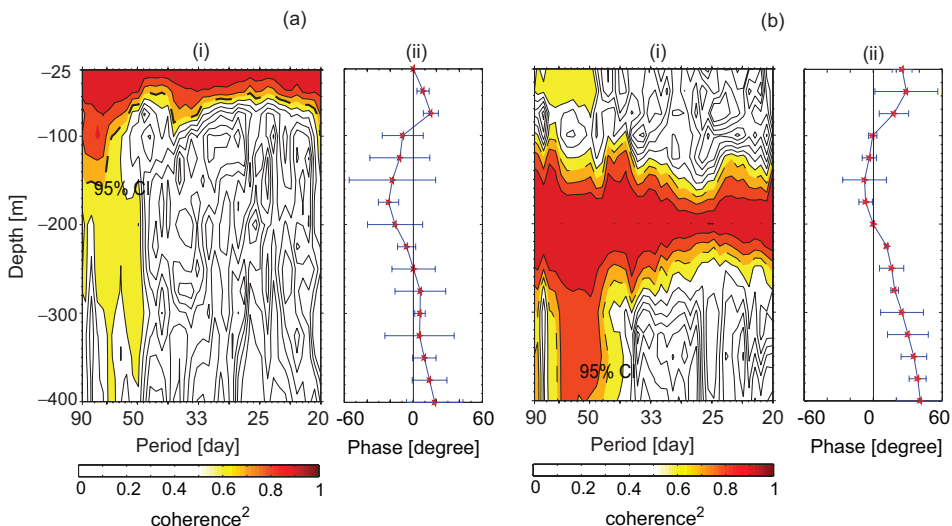


Figure 5. Coherence between the Mak-West intraseasonal along-channel flow at (a) 25 m and (b) 200 m, with the intraseasonal along-channel flow within the Mak-West thermocline. (i) Coherence squared. The dashed lines indicate the 95% significance level. (ii) Phase lags [stars]. Positive phases denote the intraseasonal along-channel flow at deeper layers leads the intraseasonal along-channel flow at a shallower depth. Error bars show the 95% confidence limits for the phase lag estimates and were computed using a Monte-Carlo scheme.

(Pedlosky, 2003). Figure 5b shows that the dominant oscillations in the lower thermocline are weakly correlated with those in the upper thermocline. As the more substantial oscillations are confined to the upper thermocline, we argue that the stratification maximum at 120 m inhibits vertical energy propagation of oscillations originating above or below that depth.

Another important characteristic observed in the lower thermocline is the strong ISV signature in May and June of both 2004 and 2005 (Fig. 2a,b). The onset of this distinct feature is consistent with the timing of a semiannual Kelvin wave forced by winds over the Indian Ocean (Sprintall *et al.*, 2000). The 2006 May–June ISV was markedly weaker. This period corresponds to a La Niña phase, when the ITF transport is increased and the thermocline deepens (Gordon *et al.*, 2008). The relatively weak intraseasonal oscillations during May–June 2006 most likely corresponds with a reduction in forcing rather than the increased viscous dissipation associated with increased vertical shear. Substantial vertical shear is observed only in the upper 100 m of Makassar Strait thermocline (Fig. 7). Since the vertical gradient of along-channel flow is significantly different from zero only within the upper thermocline, we conclude that the role of viscous dissipation is negligible in causing the differences observed between the ISV of May/June in 2004 and 2005, with that in May/June 2006 within the Makassar Strait lower thermocline.

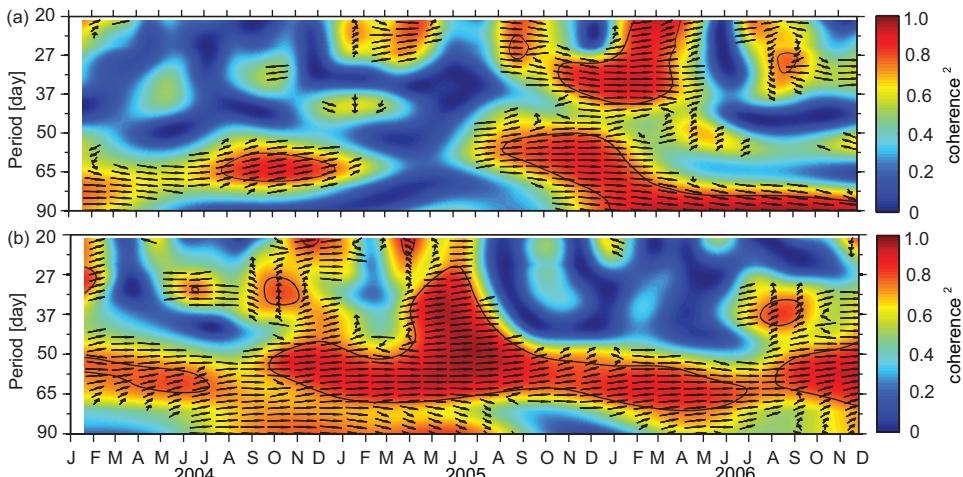


Figure 6. (a) Wavelet coherence between the intraseasonal along-channel flow at 25 m and the intraseasonal along-channel flow at 50 m observed in the Mak-West thermocline. (b) Wavelet coherence between the intraseasonal along-channel flow at 200 m and the intraseasonal along-channel flow at 350 m observed in the Mak-West thermocline. The arrows indicate the phase lags. Pointing up signifies that the along-channel flow at 50 m (350 m) leads the along-channel flow at 25 m (200 m). Pointing right denotes that the along-channel flows at 50 m (350 m) and at 25 m (200 m) are in phase. Thin black lines denote the 95% significance level.

So far, we have discussed the intraseasonal features in the upper thermocline and lower thermocline. We now investigate the common intraseasonal characteristics occupying the full range of the thermocline. A Complex Empirical Orthogonal Function [CEOF] method was applied to simplify the intricate along-channel flow observed at Mak-West mooring site into two dominant modes which accounted for 90% of total variance. The first mode explains 70% of variance within the thermocline and a wavelet transform shows it is characterized by a persistent two-month oscillation throughout the observation period (Fig. 8a). Its amplitude attains maximum value at the surface, decreases to its lowest level at 75 m, and increases toward the lower thermocline (Fig. 8c). Vertical structure of the first

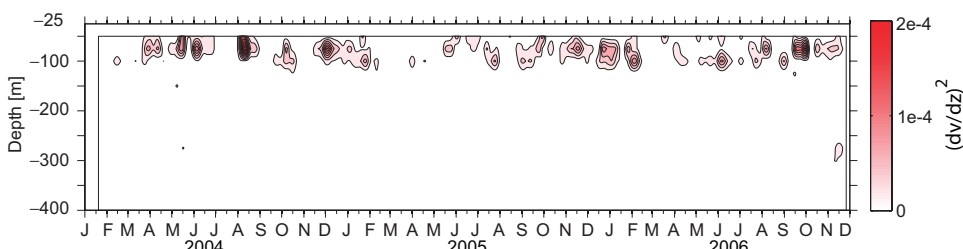


Figure 7. Squared vertical shear of interannual along-channel flow in the Mak-West thermocline.

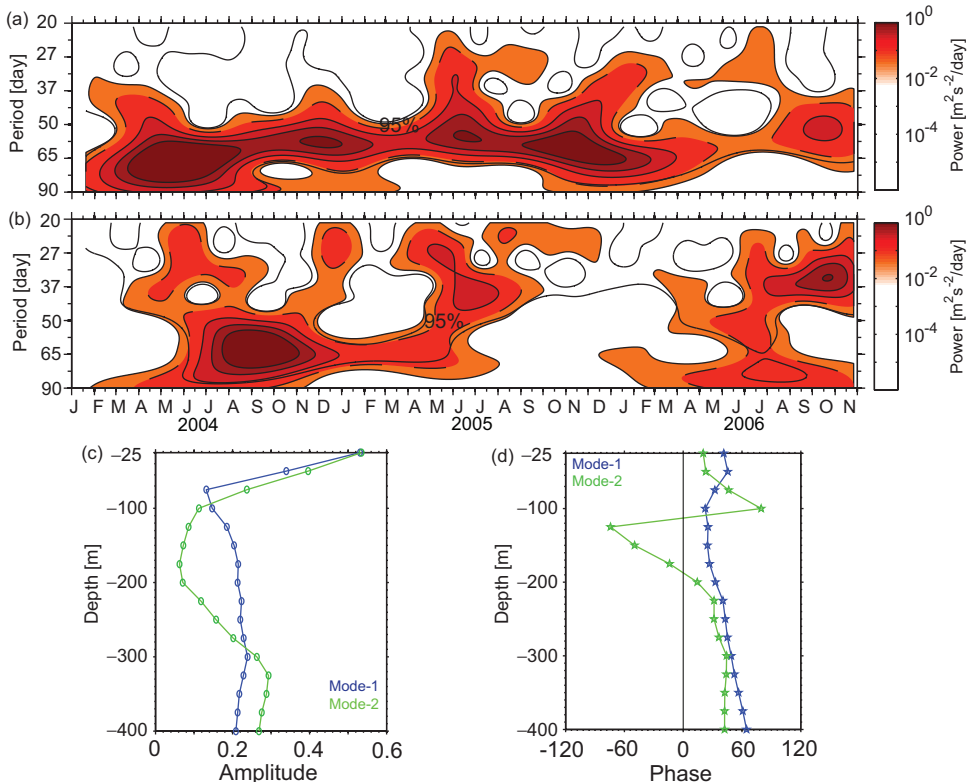


Figure 8. (a,b) Morlet Wavelet transform of the first two EOFs for the intraseasonal along-channel flow at Mak-West. The dashed lines indicate the 95% significance level. (c,d) Amplitude and phase of the first two EOFs for the intraseasonal along-channel flow at Mak-West. Modes 1 and 2 account for 70% and 20% of the variance, respectively.

two modes suggests the top thermocline depth of 25 m as a momentum source as indicated by its energetic amplitude. This large amplitude at the top thermocline level is presumably not projected farther in the thermocline layer due to viscous dissipation: Momentum transfer from the surface to deeper depths would be attenuated because substantial amount of energy is dissipated against friction due to viscosity. Instead of being further dissipated in the lower thermocline, the amplitude of the first mode increases slightly with depth down to 300 m, again indicative of downward energy propagation. As in the phase relationship for the 200 m along-channel flow ISV with deeper layers (Fig 5b, right panel), the vertical energy propagation is identified as a phase increase of $11^\circ/50$ m over the lower thermocline (Fig. 8d). This implies that it takes about two days for a 60-day oscillation to radiate its energy from 150 m to 200 m.

ii. Wind variability. The wind field in Makassar Strait, as inferred from the local meridional wind measured at Balikpapan airport, reveals a substantial amount of ISV

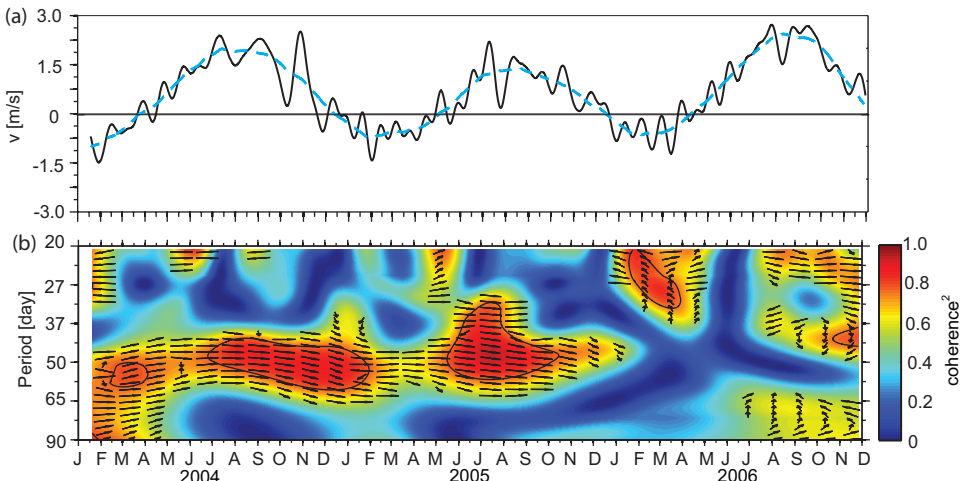


Figure 9. (a) The meridional wind monitored at the Balikpapan airport (see Figure 1 for location). Intraseasonal component of the wind (black line) modulates the seasonal cycle of the wind (dashed blue line). Negative values indicate northerly wind. The seasonal wind was obtained by applying a 90-day running mean to the full data. (b) Wavelet coherence between the intraseasonal wind at the Balikpapan airport and the intraseasonal along-channel flow at 25 m in the Mak-West thermocline. The arrows indicate the phase lags. Pointing down indicates the intraseasonal wind leads the intraseasonal flow by 90°. Pointing right signifies the wind variability and the along-channel flow are in phase. Thin black lines denote the 95% significance level.

(Fig. 9a). The seasonal cycle of local wind at Balikpapan station is driven by the monsoonal winds: northwesterly [southeasterly] winds prevail during boreal winter [summer]. On many occasions the amplitude of the meridional component of wind at intraseasonal time scales is very large, so energetic intraseasonal variations may override the seasonal cycle. Because of the nearly meridional orientation of the Labani channel, we do not include the characteristics of the zonal component of the wind in our analysis. Furthermore, the spectrum estimate of the zonal wind does not indicate any distinct peaks in ISV periods centered at 60 days, but rather, resembles a red spectrum (not shown). In contrast, meridional wind at Balikpapan airport exhibits substantial variance at 60-day oscillation (Fig. 9a). The 60-day oscillation is strong during the late summer and into the fall. A striking example of this oscillation is the anomalous southeasterly wind bursts recorded in August and October of each year, against the prevailing northwesterly monsoonal winds (Fig. 9a). In the following section, we discuss whether the atmospheric ISV is projected onto the Makassar Strait thermocline.

iii. Interaction of atmospheric and oceanic ISV. To ascertain the importance of the ISV in the atmosphere to the intraseasonal oscillations in the along-channel flow of the Makassar Strait thermocline, we employed a wavelet coherence method. The coherence shows the degree of correlation as well as how the correlation evolves with time. Again, we show

only the Mak-West data since the majority of the variance observed at Mak-East resembles that of Mak-West (Fig. 4). The strong coherence between the meridional wind and the along-channel flow at 25 m within the 45–60 days band suggests that the momentum of the atmospheric ISV is partly transferred to force the variability at the top of the Makassar Strait upper thermocline (Fig. 9b). The phase relationship (Fig. 9b) implies that the along-channel flow reaches maximum velocity 5 days following the peak of the wind, and the coherence between the wind and the flow at 25 m strengthens during summer and fall months of 2004 and 2005 but is weakened during the same period of 2006. We suspect that the deepening of the thermocline associated with the La Niña of early 2006 inhibited wind derived momentum transfer from the ocean surface to depth of 25 m and deeper layers.

Analyzing the wind influence deeper in the water column, we find that the trace of wind signatures is no longer substantially observed below 25 m (not shown). The correlation between winds and current at 50 m drops to 60%, which is below the significance level. However, the along-channel flow at 25 m is well correlated with the flow at 125 m depth (Fig. 5a). This finding suggests that the variability at intraseasonal time scales in the uppermost Makassar Strait thermocline is partly an oceanic response to energy from local wind forcing, but that the majority of ISV observed in the Makassar Strait thermocline is derived from a remote source. We now explore the potential remote sources of the Makassar Strait ISV.

b. The links between Makassar Strait ISV and Sulawesi Sea ISV

The first remote basin considered as the origin of ISV observed in Makassar Strait is Sulawesi Sea, located to the north of the INSTANT moorings (Fig. 1). The analysis of intraseasonal variations in the Sulawesi Sea inferred from mooring data is not available although mooring sites off the Pacific entrance of the Sulawesi Sea [off the southeastern tip of Mindanao Island] indicated that the 50-day oscillation is dominant (Kashino *et al.*, 1999). The study of intraseasonal oscillations in Sulawesi Sea has been done through several numerical experiments. Qiu *et al.* (1999) suggested two principle mechanisms likely responsible for the dominant 50-day oscillation in the Sulawesi Sea. First, they argued that the geometry of the Sulawesi Sea would support the intrinsic period of 50 days [the gravest Rossby wave period]. Second, the eddy shedding of the Mindanao Current was suggested to force 50-day oscillations in the Sulawesi Sea. In addition, Masumoto *et al.* (2001) hypothesized that westward propagating eddies generated at 40-days characterized the main ISV feature in the Sulawesi Sea. Both numerical experiments agreed that the ISV emanating from the Sulawesi Sea dissipated its energy along the pathway of ITF.

We examined the SLA variability measured by the Jason-1 altimetry satellite to obtain the main oscillations in Sulawesi Sea. We focused our analysis of SLA variability at 3°N and along longitudes from 118°E to 125°E in Sulawesi Sea (Fig. 1) that corresponds to the locations where the majority of the ISV variance were numerically simulated (Qiu *et al.*, 1999; Masumoto *et al.*, 2001). The intraseasonal oscillations in the Sulawesi Sea vary from 45 to 90 days and contribute significantly to the overall variance (Fig. 10a,b). Figure 10b

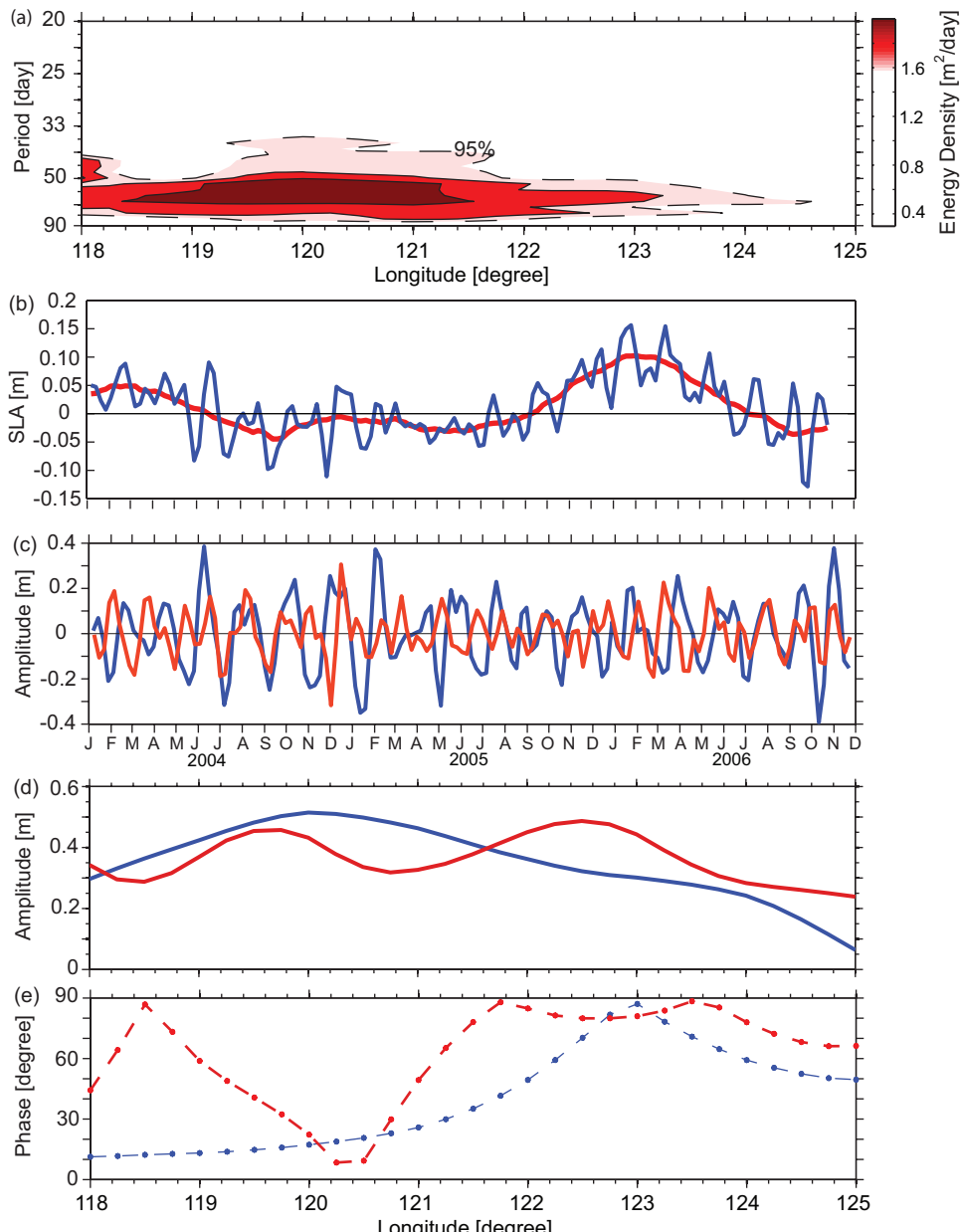


Figure 10. (a) Spectra for SLA at the intraseasonal time scales measured at 3°N ; 118°E – 125°E in the Sulawesi Sea. The dashed lines indicate the 95% significance level. (b) Intraseasonal (blue line) and seasonal (red line) SLA at 3°N ; 120°E in the Sulawesi Sea. The seasonal SLA variability was obtained by applying a 90-day running mean to the full SLA data. (c,e) CEOF analysis for SLA at the intraseasonal time scales observed at 3°N ; 118°E – 125°E in Sulawesi Sea. (c) Time series of the leading EOF modes. (d) Amplitude of the leading EOF modes. (e) Phase of the leading EOF modes. 1st and 2nd modes are in blue and red, respectively.

shows that the ISV is stronger than the seasonal variability and is of comparable strength with the interannual variability (the interannual variation was marked with a period of suppressed [enhanced] SLA anomaly linked to a phase of a weak El Niño [La Niña]). The spatial variability of the ISV signature indicates the amplification towards the western boundary of the Sulawesi Sea (Fig. 10a).

To further analyze the ISV characteristics in Sulawesi Sea, a CEOF method was applied to extract the most common pattern governing the SLA variability at intraseasonal time scales. The amplitude time series of the ISV patterns that accounts for 90% of the total intraseasonal SLA variance are given in Figure 10c. The leading mode, which explains 70% variance, reveals the importance of the 45–90 day variability as the dominant intraseasonal oscillation, and its zonal structure supports the energy intensification towards the western boundary of Sulawesi Sea (Fig. 10d). The second mode, associated with the 20% of total variance, reveals another band of 30–40 day energy. The dominance of the 45–90 day and 30–40 day periods may be the expression of the cyclonic eddies which were well resolved in the numerical experiments of Qiu *et al.* (1999) and Masumoto *et al.* (2001). By analyzing the relative phase lags at several longitudes for the first orthogonal mode (Fig. 10e), we argue that the 50-day oscillation propagates westward at a phase speed of 0.2 m/s which is similar to the phase speed of a baroclinic Rossby wave as simulated through the numerical experiments (Qiu *et al.*, 1999; Masumoto *et al.*, 2001).

To investigate whether the variability at the intraseasonal time scales observed in the Sulawesi Sea is related to the variability in Makassar Strait, we correlate SLA in the Sulawesi Sea and the along-channel flow in Makassar Strait (Fig. 11). The dominant intraseasonal variability of the Sulawesi Sea SLA correlates significantly with the Makassar thermocline layer variability. The most coherent fluctuations of the Sulawesi and Makassar Strait ISV are within the period band of 50–70 days. The corresponding analysis of relative phase difference of the most coherent variability confirms that the features emanating from the Sulawesi Sea propagate and radiate energy into Makassar Strait with phase speeds of 0.2–0.3 m/s (Fig. 11, right panel). Thorough discussion on the mechanisms or forms through which the energy originating from the Sulawesi Sea propagates into Makassar Strait is not within the framework of our present study, but will be investigated in the future.

c. Links between ISV in Makassar Strait and ISV in Lombok Strait and EEIO

Lombok Strait throughflow displays substantial intraseasonal variability (Arief and Murray, 1996; Wijffels and Meyers, 2004; Sprintall *et al.*, 2009). The remote wind fields, particularly wind variability in the equatorial Indian Ocean, are identified as the source of the ISV in Lombok Strait. Here we investigate the linkage of Lombok ISV to that of Makassar using the INSTANT data in Lombok Strait.

In the upper thermocline, the dominant intraseasonal fluctuations in Lombok Strait are more energetic than in Makassar Strait (Fig. 12a). A wavelet-coherence revealed that the 60–90 day oscillations observed at both straits are coherent with a phase relationship that

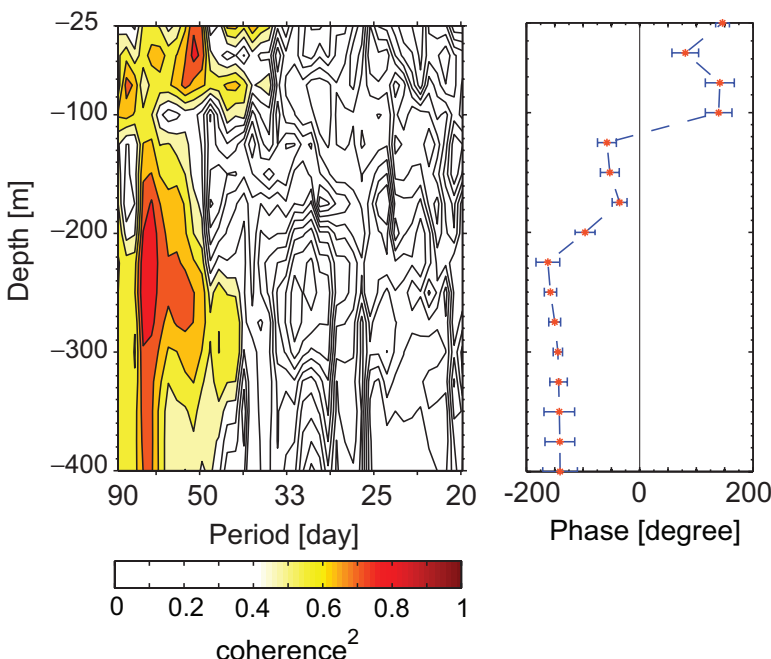


Figure 11. Coherence between the intraseasonal SLA in Sulawesi Sea and the intraseasonal along-channel flow from Mak-West. [Left panel]: Coherence squared. The dashed lines indicate the 95% significance level. [Right Panel]: Phase lags [stars]. Negative phases denote the intraseasonal SLA leads the intraseasonal along-channel flow. Error bars show the 95% confidence limits for the phase lag estimates and were computed using a Monte-Carlo scheme.

suggests a phase shift of about 40° (Fig. 12b), suggesting a feature that radiates toward Makassar Strait at speeds of 1–1.5 m/s. By applying the Liouville-Green approximation (Gill, 1982) to the stratification profile in Makassar Strait (Fig. 3), we find theoretical phase speeds of internal waves for the lowest three ocean modes are 1.4 m/s, 0.7 m/s, and 0.5 m/s, respectively. The phase speed of 1–1.5 m/s is commensurate with the first mode of baroclinic wave speed in a continuously stratified ocean. To investigate the possibility of a baroclinic wave propagating from Lombok Strait to Makassar Strait, we compute the theoretical lower bound of the coastal trapping period. The coastal trapping period, $T = \frac{4\pi}{\beta R_m}$ (Allen and Romea, 1980), is a preliminary approach to estimate the longest period of any coastal trapped waves possibly excited at a certain location. The coastal trapping period (T) is inversely proportional to the internal Rossby radius of deformation [R_m] and the variation of the Coriolis parameter with latitude (β). The baroclinic Rossby radius of deformation is a function of phase speed [c] and Coriolis parameter [f], and defined as $R_m = \frac{c}{f}$ (Gill, 1982; Pedlosky, 2003). We specified c in both Makassar Strait and Lombok Strait to be 1 m s^{-1} , the phase speed of a propagating feature inferred from

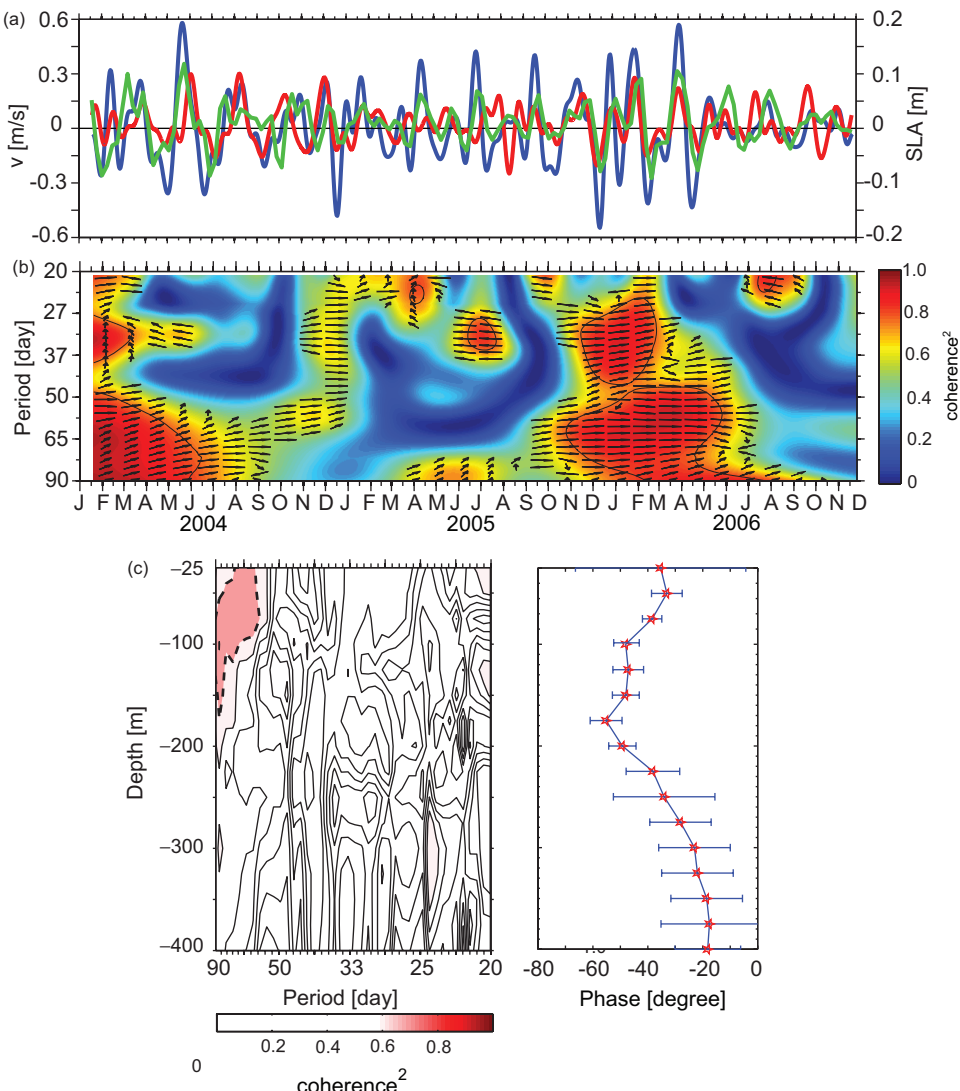


Figure 12. (a) Along-channel flow at the intraseasonal time scales measured at 50 m from Mak-West (red line) and from Lom-East (blue line), and SLA at the intraseasonal time scales from Lom-East (green line). (b) Wavelet coherence between ISV at 50 m from Mak-West and ISV at 50 m from Lom-East. The arrows indicate the phase lags: Pointing up indicates ISV at Lom-East leads ISV at Mak-West by 90°. Pointing right signifies intraseasonal oscillations at Mak-West and at Lom-East are in phase. Thin black lines denote the 95% significance level. (c) Coherence between ISV at 50 m from Lom-East and ISV in the Mak-West thermocline. [Left panel]: Coherence squared. The dashed lines indicate the 95% coherence significance level. [Right Panel]: Phase lags [stars]. Negative phases denote ISV at Lom-East leads ISV at Mak-West. Error bars show the 95% confidence limits of the phase lag estimates and are computed using a Monte-Carlo scheme.

observation. Using the given phase speed, $f_m = 7.5 \times 10^{-6} \text{ s}^{-1}$, $f_l = 2.1 \times 10^{-5} \text{ s}^{-1}$, $\beta_m = 2.3 \times 10^{-11} \text{ m}^{-1} \text{ s}^{-1}$, and $\beta_l = 2.28 \times 10^{-11} \text{ m}^{-1} \text{ s}^{-1}$ [subscripts m and l denote Makassar and Lombok respectively], we determined that the theoretical lower bounds of the coastal trapping period in Makassar and Lombok Strait are 50 days and 129 days, respectively. This suggests that the coherent 60-day oscillation observed in Lombok Strait can reasonably be classified as a baroclinic CTKW. Further evidence of the CTKW expression is that the upper thermocline along-channel flow in Lombok Strait is in geostrophic balance, as indicated through the surge [drop] of SLA corresponding to the northward [southward] along-channel flow (Fig. 12a).

On the other hand, it is likely that the 60-day variability observed in the upper thermocline of Makassar Strait is not a trapped wave feature since its longest theoretical period at the Makassar moorings is 50 days, and another waveform such as baroclinic topographic Rossby waves plausibly transmit the energy from Lombok Strait. McCreary (1984) suggested that an equatorial Rossby wave would propagate vertically at an angle of $\theta = \pm \tan^{-1}\left(\frac{N}{\omega(2l+1)}\right)$ where l is the wave mode. Provided $N = 0.0123 \text{ s}^{-1}$ [the largest N value observed in Makassar Strait, see Fig. 3], $l = 1$ [first mode of a baroclinic wave], a distance of 673 km separating Lombok and Makassar moorings, a baroclinic wave oscillating at a period band of 60–90 days and emanating from the Lombok Strait surface would penetrate vertically into the Makassar Strait thermocline within a depth range of 130–200 m. The moorings data reveal that wave vertical propagation is evident as indicated by the strong coherency between the dominant variability at 50 m depth in Lombok Strait and that of the Makassar Strait upper thermocline (Fig. 12c). It is inferred from the phase relationship (Fig. 12c) that the energy propagates vertically from 50 m depth in Lombok Strait to the Makassar Strait mid-thermocline although its signature weakens in the lower thermocline. The strong coherence between the dominant flow at 50 m depth in Lombok Strait and that of the Makassar Strait upper thermocline and the vertical propagation from Lombok Strait to Makassar Strait may indicate that baroclinic Rossby wave dynamics are applicable as a first approximation to describe how the energy of 60–90 day variability is transmitted from Lombok Strait to Makassar Strait.

As previously mentioned, the dominant oscillations at 50 m depth in the upper thermocline in Makassar Strait are not as strong as that in Lombok Strait. The attenuation of the 45–90 days energy in Makassar Strait is probably due to the spreading of the horizontal wave scale associated with the growth of internal Rossby deformation radius [R_m] toward the equator. Given $R_{1m} = 275 \text{ km}$ and $R_{1l} = 66 \text{ km}$, the ratio between the internal Rossby radii in Makassar to Lombok Strait is three, leading to the amplification of the horizontal wave scale in Makassar Strait. By conservation of energy flux, the amplification of the horizontal wave scale in Makassar Strait leads to decrease of the wave amplitude, as reflected in the weakening of the along-channel speed in Makassar Strait. Another possible mechanism related to the attenuation of the 45–90 day energy in Makassar Strait is that the wave path is not only from Lombok Strait to Makassar Strait, but

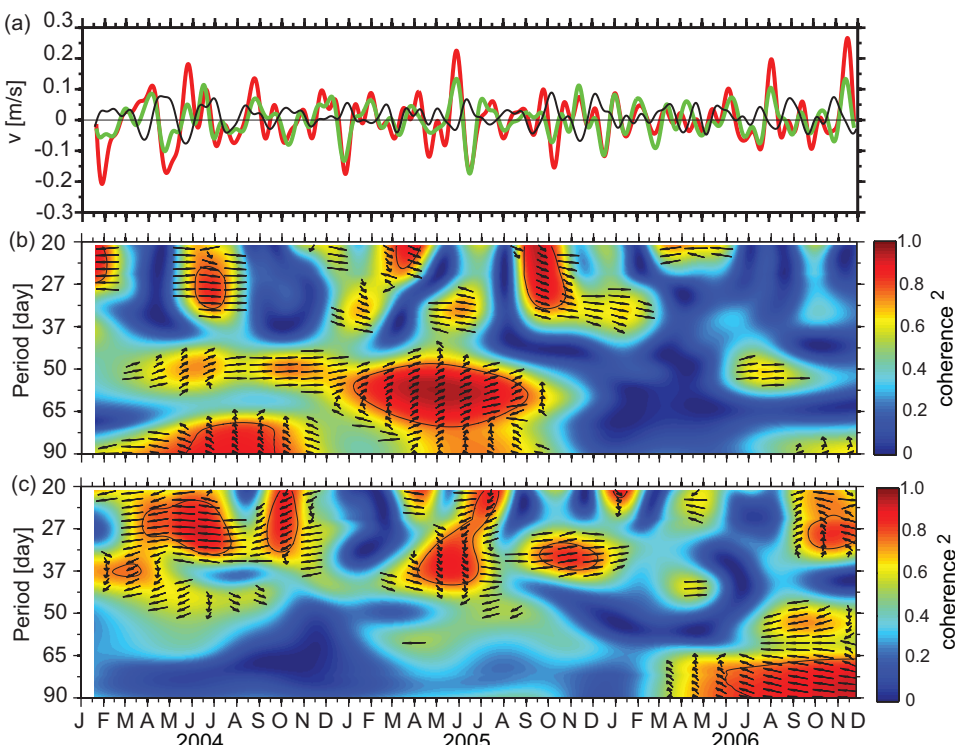


Figure 13. (a) Intraseasonal along-channel flow at 350 m from Lom-East (green line) and Mak-West (red line). Black lines indicate the intraseasonal zonal velocity at 350 m from the EEIO mooring. (b) Wavelet coherence between ISV at 350 m from Lom-East and ISV at 350 m from Mak-West. The arrows indicate the phase lags: Pointing up means ISV at Lom-East leads ISV at Mak-West by 90°; Pointing right signifies intraseasonal oscillations at Mak-West and at Lom-East are in phase. (c) Wavelet coherence between ISV at 350 m from EEIO and ISV at 350 m from Lom-East. The arrows indicate the phase lags: Pointing up means ISV at EEIO leads ISV at Lom-East by 90°; Pointing right signifies ISV at Lom-East and ISV at EEIO are in phase. Thin black lines denote the 95% significance level.

also from Lombok Strait to Java Sea and to Flores Sea (Fig. 1). In other words, a baroclinic wave in Lombok Strait could possibly scatter its energy into three different outlets: Java Sea, Flores Sea, and Makassar Strait leading to the observed weaker along-channel flow in Makassar Strait.

In the lower thermocline of Lombok Strait at 350 m, the variance is less energetic than at 350 m depth in Makassar Strait (Fig. 13a). Nevertheless the dominant fluctuations observed at 350 m in Lombok and in Makassar Strait are coherent, particularly in the 45–55 days band from January to September 2005 (Fig. 13b). The phase shift of the coherent oscillations indicates the propagation of a non-dispersive perturbation towards Makassar Strait with a phase speed of 1 m/s. The coherent motion found at 350 m is well

below the Lombok sill depth of ~ 300 m located to the south of the Lom-East mooring (Fig. 1) such that its characteristics are likely influenced by the sill's presence. The sill would act to block energy transmission from the Indian Ocean toward Makassar Strait for all oscillations occupying the water column below the sill depth. Correlation of the zonal velocity at 350 m in the EEIO with the along-channel flow at 350 m in Lombok Strait revealed that there is no significant coherence at 45–55 day periods for almost the entire observation period, except during the last 6 months in 2006 (Fig. 13c). The effect of Lombok Strait sill coupled with the thermocline vertical motion at interannual timescales might explain the lower thermocline ISV modulation by ENSO. As discussed in Section 3a(i) and shown in Figure 13b, the ISV signature in Lombok and Makassar Straits was markedly weaker in May–June 2006 during a weak La Niña period. The less energetic ISV is partly due to the increased effectiveness of Lombok Strait sill in blocking the incoming energy when the thermocline dips in a La Niña phase. In contrast, the effect of Lombok Strait sill would not be as strong when the temperature cools and the lower thermocline thickens during an El Niño phase such as in May/June 2005 when the coherence between Lombok and Makassar at 350 m depth is significant (Fig 13b). Therefore, it is reasonable to argue that the sill in Lombok Strait acts as an obstacle for the energy from the Indian Ocean transmitted into the internal of Indonesian seas.

4. Summary

The intraseasonal variability [ISV] in the Makassar Strait thermocline and its linkage to the variability in the surrounding seas are investigated. The Makassar along-channel ISV as observed at the Mak-West and Mak-East moorings is characterized by 45–90 day oscillations, derived from either the local wind fluctuations in the surface layer or from more remote sources within the thermocline. Atmospheric ISV exhibits a substantial role in modulating or on some occasions fully over-riding the seasonal cycle. The oceanic ISV on the other hand exhibits western intensification, and is vertically and horizontally coherent with downward energy propagation speeds of 25 m/day. The stratification contributes substantially to the vertical distribution of the oceanic ISV signatures. For example, excessive buoyancy flux into Makassar Strait combined with a deeper thermocline characteristic of a La Niña period play a major role in inhibiting ISV momentum transfer from the base of the mixed layer to deeper within the water column. We argue that local wind variability partly transfers its momentum to force ISV within the upper 25 m of Makassar Strait. However, the vertically coherent intraseasonal fluctuations within the thermocline are unlikely associated with the local atmospheric variation, but they are substantially related to the remotely perturbed forcing.

Investigating the relation between ISV in Makassar Strait thermocline and ISV in the Sulawesi Sea and Lombok Strait, it is inferred that in the upper thermocline, a baroclinic wave radiating from 50 m depth in Lombok Strait at a slight angle is suspected to force the variability at periods of 60–90 days in Makassar Strait. Adding further complexity, deep reaching 50–70 day oscillations originating in the Sulawesi Sea make up the full picture of

the intraseasonal features recorded in the Makassar Strait thermocline. The nature of the ISV also reveals its dependence on ENSO and the monsoon phase. An El Niño episode dampens the strong shear that is confined to the upper thermocline, while the La Niña phase attenuates the energetic ISV during the monsoon-transition period in the lower thermocline. Upper thermocline and lower thermocline ISV are not synchronous with the ENSO phases: during El Niño, the ISV is suppressed in the upper thermocline and intensified in the lower thermocline. The nonconformity might indicate that the lower thermocline ISV draws some of its momentum from the equatorial Indian Ocean ISV transmitted through Lombok Strait. How the ISV in Makassar Strait thermocline is dynamically related to the equatorial Kelvin waves in the Indian Ocean and its intricate interplay with the deep reaching features in the Sulawesi Sea that force variability in the subthermocline is further addressed in ongoing studies.

Acknowledgments. This work was supported by the National Science Foundation grant OCE-0219782, OCE-0725935, and OCE-0725476 (JS). The authors thank Dr. Yukio Masumoto [Japan Agency for Marine-Earth Science and Technology/JAMSTEC] and Indra Gustari M.Sc [Badan Meteorologi, Klimatologi dan Geofisika/BMKG] for providing the zonal current data in the eastern equatorial Indian Ocean and the atmospheric variables observed at Balikpapan Airport respectively. Bruce Huber is acknowledged for helping with the preparation of the gridded along-channel flow datasets in Makassar Strait. Gratitude is extended to Dr. K. H. Brink and two anonymous reviewers for their constructive comments. This is Lamont-Doherty contribution number 7321.

REFERENCES

- Allen J. S. and R. D. Romea. 1980. On coastal trapped waves at low latitude in a stratified ocean. *J. Fluid Mech.*, 98, 555–585.
- Arief, D. and S. P. Murray. 1996. Low frequency fluctuations in the Indonesian throughflow through Lombok Strait. *J. Geophys. Res.*, 101, 12,455–12,464.
- Cravette, S., J. Boulanger and J. Picaut. 2004. Reflection of intraseasonal equatorial Rossby waves at the western boundary of the Pacific Ocean. *Geophys. Res. Lett.*, 31, L10301, doi: 10.1029/2004GL019679.
- Ffield, A., K. Vranes, A. L. Gordon, R. D. Susanto and S. L. Garzoli. 2000. Temperature variability within Makassar Strait. *Geophys. Res. Lett.*, 27, 237–240.
- Fisher, N. I., T. Lewis and B. J. J. Embleton. 1987. Statistical Analysis of Spherical Data, Cambridge University Press, 329 pp.
- Gill, A. E. 1982. Atmosphere-Ocean Dynamics, Academic Press, NY, 662 pp.
- Gordon, A. L. and R. A. Fine. 1996. Pathways of water between the Pacific and Indian oceans in the Indonesian seas. *Nature*, 379, 146–149.
- Gordon, A. L., R. D. Susanto and A. Ffield. 1999. Throughflow within Makassar Strait. *Geophys. Res. Lett.*, 26, 3325–3328.
- Gordon, A. L., R. D. Susanto, A. Ffield, B. A. Huber, W. Pranowo and S. Wirasantosa. 2008. Makassar Strait Throughflow, 2004 to 2006. *Geophys. Res. Lett.*, 35, doi: 10.1029/2008GL036372.
- Iskandar, I., W. Mardiansyah, Y. Masumoto and T. Yamagata. 2005. Intraseasonal Kelvin waves along the southern coast of Sumatra and Java. *J. Geophys. Res.*, 110, C04013, doi: 10.1029/2004JC00250.
- Jenkins, G. M. and D. G. Watts. 1969. Spectral Analysis and Its Applications, Holden-Day, 379–381.

- Kashino, Y., H. Watanabe, B. Herunadi, M. Aoayama and D. Hartoyo. 1999. Current variability at the Pacific entrance of the Indonesian Throughflow. *J. Geophys. Res.*, *104*, 11021–11035.
- Madden, R. A. and P. R. Julian. 1971. Detection of a 40–50 day oscillation in the zonal wind in the tropical Pacific. *J. Atmos. Sci.*, *28*, 702–708.
- Masumoto, Y., H. Hase, Y. Kuroda, H. Matsuura and K. Takeuchi. 2005. Intraseasonal variability in the upper layer currents observed in the eastern equatorial Indian Ocean. *Geophys. Res. Lett.*, *32*, L02607, doi:10.1029/2004GRL21896.
- Masumoto, Y., T. Kagimoto, M. Yoshida, M. Fukuda, N. Hirose and T. Yamagata. 2001. Intraseasonal eddies in the Sulawesi Sea simulated in an ocean general circulation model. *Geophys. Res. Lett.*, *28*, 1631–1634.
- McBride, J. L. and W. M. Frank. 1996. Relationships between stability and monsoon convection. *J. Atmos. Sci.*, *56*, 24–36.
- McCreary, J. 1984. Equatorial beams. *J. Mar. Res.*, *42*, 395–430.
- Pedlosky, J. 2003. Waves in the Ocean and Atmosphere, Springer-Verlaag, 276 pp.
- Percival, D. B. and A. T. Walden. 1993. Spectral Analysis for Physical Applications, Multitaper and Conventional Univariate Techniques, Cambridge University Press, 583 pp.
- Qiu, B., M. Mao and Y. Kashino. 1999. Intraseasonal variability in the Indo-Pacific throughflow and the regions surrounding the Indonesian Seas. *J. Phys. Oceanogr.*, *29*, 1599–1618.
- Qu, T., J. Gan, A. Ishida, Y. Kashino and T. Tozuka. 2008. Semiannual variation in the western tropical Pacific Ocean. *Geophys. Res. Lett.*, *35*, L16602, doi: 10.1029/2008GL035058.
- Sprintall, J., A. L. Gordon, R. Murtugudde and R. Dwi Susanto. 2000. A semiannual Indian Ocean forced Kelvin wave observed in the Indonesian seas in May 1997. *J. Geophys. Res.*, *105*, 17, 217–230.
- Sprintall, J., S. Wijffels, A. L. Gordon, A. Ffield, R. Molcard, R. Dwi Susanto, I. Soesilo, J. Sopaheluwakan, Y. Surachman and H. Van Aken. 2004. INSTANT: A new international array to measure the Indonesian Throughflow. *EOS Transactions*, *85*, 369.
- Sprintall, J., S. Wijffels, R. Molcard and Indra Jaya. 2009. Direct estimates of Indonesian Throughflow entering the Indian Ocean: 2004–2006, *J. Geophys. Res.*, *114*, C07001, doi: 10.1029/2008JC005257.
- Susanto, R. D., A. L. Gordon, J. Sprintall and B. Herunadi. 2000. Intraseasonal variability and tides in Makassar Strait. *Geophys. Res. Lett.*, *27*, 1499–1502.
- Syamsudin, F., A. Kaneko and D. B. Haidvogel. 2004. Numerical and observational estimates of Indian Ocean Kelvin wave intrusion into Lombok Strait. *Geophys. Res. Lett.*, *31*, L24307, doi: 10.1029/2004GL021227.
- Thompson, R. O. R. Y. 1979. Coherence significance levels. *J. Atmos. Sci.*, *36*, 2020–2021.
- Wheeler, M., G. N. Kiladis and P. J. Webster. 2000. Large-scale dynamical fields associated with convectively coupled equatorial waves. *J. Atmos. Sci.*, *57*, 613–640.
- Wijffels, S. and G. Meyers. 2004. An intersection of oceanic waveguides: Variability in the Indonesian Throughflow region. *J. Phys. Oceanogr.*, *34*, 1232–1253.

Received: 12 May, 2009; revised: 11 January, 2010.